

# A Three-Pronged Computational Approach for Evaluating Density Based Semi Empirical Equations of Supercritical Extraction Process and Data

Srinidhi Srinidhi<sup>1,2</sup>

1. Department of Chemical and Biological Engineering, School of Engineering and Applied Sciences

2. University at Buffalo, State University of New York

## Abstract

Software programs for parameter estimation, phase visualization and predictive modeling of supercritical extraction process and data using algorithms is presented in this work. A contextually appropriate, iterative, ordinary least squares estimation and selection method is developed for estimating model coefficients of density based semi empirical model equations associated with this process and data. Visualization of the phase behaviors projected by the specific density based semiempirical model equation(s) is also performed iteratively by plotting three-dimensional surfaces involving the state variables and solute solubility mole fraction. Predictive modeling of input empirical data has been implemented using three supervised machine learning algorithms (Multilayer perceptron, K-nearest neighbors and Support vector regression). Hyperparameter optimization of the machine learning algorithms is performed prior to prediction. Detailed analysis of the prediction is conducted by using standard scoring metrics and descriptive charts. Theoretical inference and discrepancies regarding the predicted window of maximum/optimal solubility, modeling efficiency, vapor liquid equilibrium and phase behaviors projected by the model equations have been elucidated from the program outputs. In summary, these programs are unique, accurate, reliable and simple computational tools for evaluating/designing density based semiempirical equation(s) of supercritical extraction process and associated data.

## Keywords

Supercritical Extraction, Density Based Semiempirical Equations, Computational Modeling Tools, Machine Learning

# **1 A Three-Pronged Computational Approach for Evaluating Density Based 2 Semi Empirical Equations of Supercritical Extraction Process and Data**

Srinidhi<sup>1,\*</sup>

<sup>1</sup>*Department of Chemical and Biological Engineering, School of Engineering and Applied Sciences, The State University of New York at Buffalo, Buffalo, NY 14260.*

\*Corresponding author, e-mail: [srnidh2@buffalo.edu](mailto:srinidh2@buffalo.edu) ; [msrinidhi2@gmail.com](mailto:msrinidhi2@gmail.com)

ORCID: [0000-0002-5318-8639](#) ;

14

## Abstract

15

16 Software programs for parameter estimation, phase visualization and predictive  
17 modeling of supercritical extraction process and data using algorithms is presented in this work.  
18 A contextually appropriate, iterative, ordinary least squares estimation and selection method is  
19 developed for estimating model coefficients of density based semi empirical model equations  
20 associated with this process and data. Visualization of the phase behaviors projected by the  
21 specific density based semiempirical model equation(s) is also performed iteratively by plotting  
22 three-dimensional surfaces involving the state variables and solute solubility mole fraction.  
23 Predictive modeling of input empirical data has been implemented using three supervised  
24 machine learning algorithms (Multilayer perceptron, K-nearest neighbors and Support vector  
25 regression). Hyperparameter optimization of the machine learning algorithms is performed  
26 prior to prediction. Detailed analysis of the prediction is conducted by using standard scoring  
27 metrics and descriptive charts. Theoretical inference and discrepancies regarding the predicted  
28 window of maximum/optimal solubility, modeling efficiency, vapor liquid equilibrium and  
29 phase behaviors projected by the model equations have been elucidated from the program  
30 outputs. In summary, these programs are unique, accurate, reliable and simple computational  
31 tools for evaluating/designing density based semiempirical equation(s) of supercritical  
32 extraction process and associated data.

33

34 **Keywords:** Parameter Estimation, Phase Visualization, Predictive modeling, Ordinary Least  
35 Squares, Machine Learning.

36

## Introduction

38

39 Theoretical, Empirical and Semi empirical Models are being developed and studied for  
40 modeling and understanding Super/subcritical fluid extraction processes (Huang et al. 2012;  
41 Rai et al. 2014). In particular, Density based Semiempirical model equations (DBSE Model  
42 Equations) are very popular and are being designed for modeling this process and therefore is  
43 part of a growing body of research (Hawthorne 1990; Herrero et al. 2010; Knez et al. 2013;  
44 Alwi and Garlapati 2021a).

45 Novel DBSE models are developed with the aim to capture (approximate) and reproduce data  
46 specific non linearity and complexity (dynamic and non-dynamic behavior) in the process.

47 Modeling in this scenario is primarily focused on the operating range of the process parameters

48 observed during desired output/yield levels (Tabernero et al. 2010). Unfortunately, in most  
49 cases, this window (presumably rich in information) is narrow and is solute/process specific.  
50 Almost every study describing a novel DBSE model have proceeded by distilling facts about  
51 the variation in solvating power observed in the process and drawing fundamental relations  
52 (from similar studies) between the operating process parameters and the dependent variable  
53 [ $\ln(y)$ , T, P, D]. A good and elegant example for this is the study and model presented by  
54 (Asgarpour Khansary et al. 2015). Least squares modeling is a subclass of Black box modeling  
55 and has been extensively employed for estimating model parameters, their confidence regions  
56 (Bounds/Intervals) and importantly for identifying causation of variance in linear models.  
57 Herein, Ordinary least squares estimation method is used for estimating parameter coefficients  
58 (and their confidence regions) present in DBSE Model equations (Lakshmi et al. 2021).  
59 Further, A necessary requirement for the design of DBSE models is the qualitative and  
60 quantitative knowledge of phase behavior of components in the reaction mix during the process.  
61 Phase diagrams illustrate important differentials in vapor pressure curves of pure CO<sub>2</sub> and other  
62 reaction components in the presence of solutes. This information is crucial for accurately  
63 identifying operating conditions wherein melting of the reaction mix leading to a desirable  
64 solute rich liquid phase occurs. In essence, phase diagrams are central to the process of finding  
65 regions (boundaries) of importance in the P-T-D-x (Pressure-Temperature-Density-solute  
66 solubility mole fraction) projections, wherein separations and extraction is actually possible  
67 (and feasible) and occurs in reality (Bartle et al. 1991). These regions (phase/parameter  
68 boundaries) depict equilibrium planes and latency of reaction mix that aid in process design and  
69 this is considered as a multifaceted and multi-attribute dependent endeavour. These attributes  
70 can be and are not limited to,

- 71 1. Regions where solvent compression occurs leading to repulsive solute-solvent  
72 interactions causing undesired immiscibility.
- 73 2. Regions where two-phase retrograde condensation/crystallization occurs near the lower  
74 and upper crossover regions/planes/edges.
- 75 3. Regions (edges/paths/points/trajectories) depicting the component(s) latency (phase  
76 change), chemical potential thermal stability of the solute leading to variations in  
77 solvating power/effect. Physical properties of solutes vary widely and significantly  
78 amount to differences during solute solubility prediction.

79 Machine learning algorithms, in recent years, are gaining importance and are being developed  
80 for predictive modeling for engineering applications. ML algorithms can accommodate

81 (consider) ‘n’ number of parameters, and therefore can predictively model processes with  
82 desired tolerance, precision and accuracy. Invaluable for accountability and research  
83 applications, hyperparameters associated with ML algorithms offers the choice of model  
84 optimization and validation. Standardized ML algorithms are applied to model a multitude of  
85 phenomena/processes in Engineering (Selvaratnam and Koodali 2021). Therefore, with the fast  
86 parametrization and modeling of analytical and industrial processes, supervised learning  
87 models like, Regression, Multilayer Perceptron, Support Vector Machine and K-nearest  
88 neighbours are (can also be) specially applied to these processes. For Chemistry and Chemical  
89 Engineering applications, A number of Software program packages based on supervised  
90 learning are already available and are always under continuous development (Khatib and de  
91 Jong 2020). In recent years, estimating/predicting solute solubility during the supercritical fluid  
92 extraction is gaining importance and necessitates predictive modeling of this process (Butler et  
93 al. 2018; Schweidtmann et al. 2021; Roach et al. 2023). The reliable and utilitarian software  
94 program can be used to accurately describe extant pattern and behavior in the measured data  
95 associated with this process and possibly beyond the regions and scope of this measured  
96 empirical data for reaching higher levels of process interpretation and accurate predictive  
97 capabilities. With this as the goal, the predictive modeling program described here has been  
98 written and focused to meet this expectation(s). Further, the complete work (workflow)  
99 presented here, is also designed for visualization and for explicating the phase behavior of  
100 existing (and newer) model equations and for evaluating the boundedness of the estimated  
101 parameter space. This workflow is holistic and is particularly useful for designing newer,  
102 efficient (accurate and precise) equations heuristically. Conveniently, As previously mentioned,  
103 a one-time-run-all code has been provided for implementing state-of-the-art machine learning  
104 algorithms for predictive modeling of DBSE model equation associated data. When correctly  
105 deployed, this work could potentially reach the helm of this growing body of research from this  
106 three-pronged computational modeling approach. To summarize, the programs are stand alone,  
107 simple, unique, computationally economic and are also easy to implement. The objectives and  
108 Software being postured here in this article are listed below,

- 109 1. A MATLAB program for estimating and comparatively analysing, parameters of  
110 extant/newly developed density based semi empirical model equations of supercritical  
111 fluid extraction process comprising of variables [ $\ln(y)$ , T, P, D] using ordinary least  
112 squares parameter estimation method.
- 113 2. A MATLAB program for visualizing parameter profiles and Phase behaviors of DBSE  
114 model equations using 3D surface plots.

- 115 3. A Python based Jupyter Notebook for implementing supervised machine learning  
 116 algorithms (Multilayer Perceptron, K nearest neighbours and Support vector machines)  
 117 based on experimental data involving the variables (Temperature (T), Pressure (P),  
 118 Density (D) and Solute solubility Mole fraction (y)).
- 119 4. Provide concluding remarks about the program scripts, its usage and availability.

120 **Experimental**

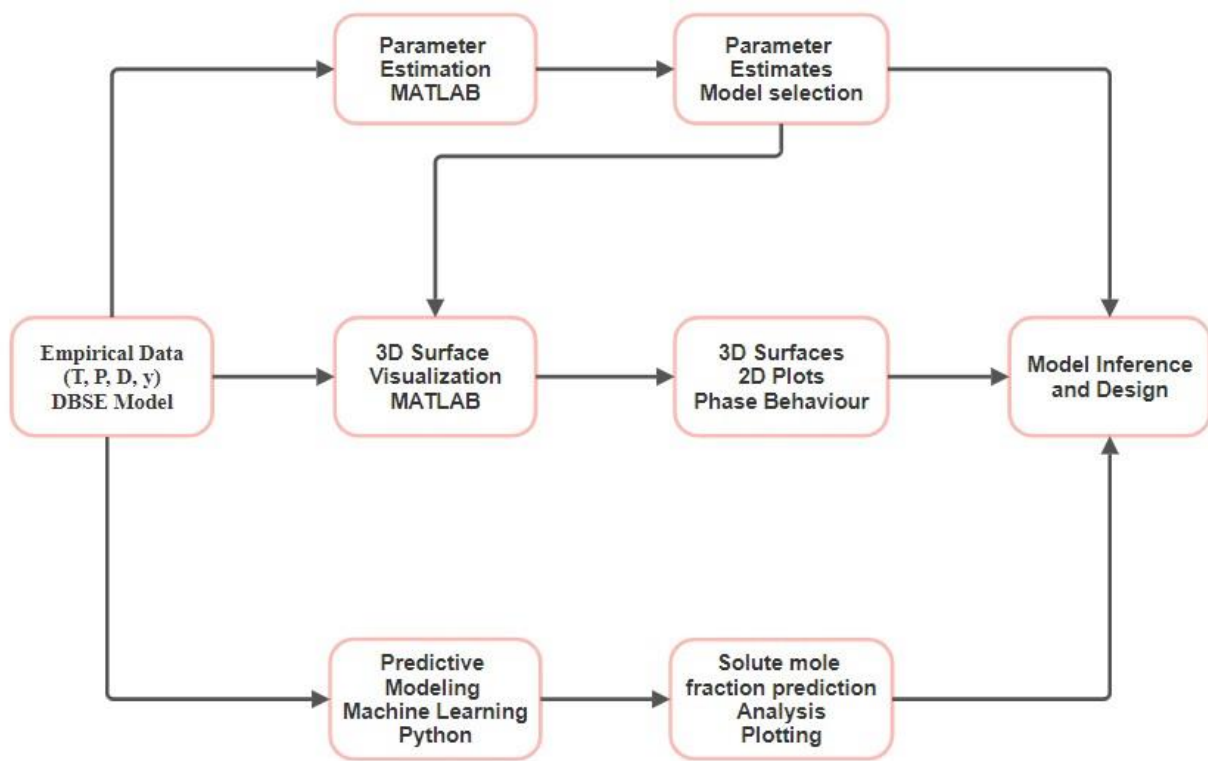
122 **Description of Data: Input Matrices and Parameter Description**

123

124 The MATLAB (Matlab 1984) and Python program scripts presented in this work requires two  
 125 input matrices. First, Consider, the Input data as a matrix where in,  $Data \in R^n$  and  $n \in Z$ ,  
 126 then,

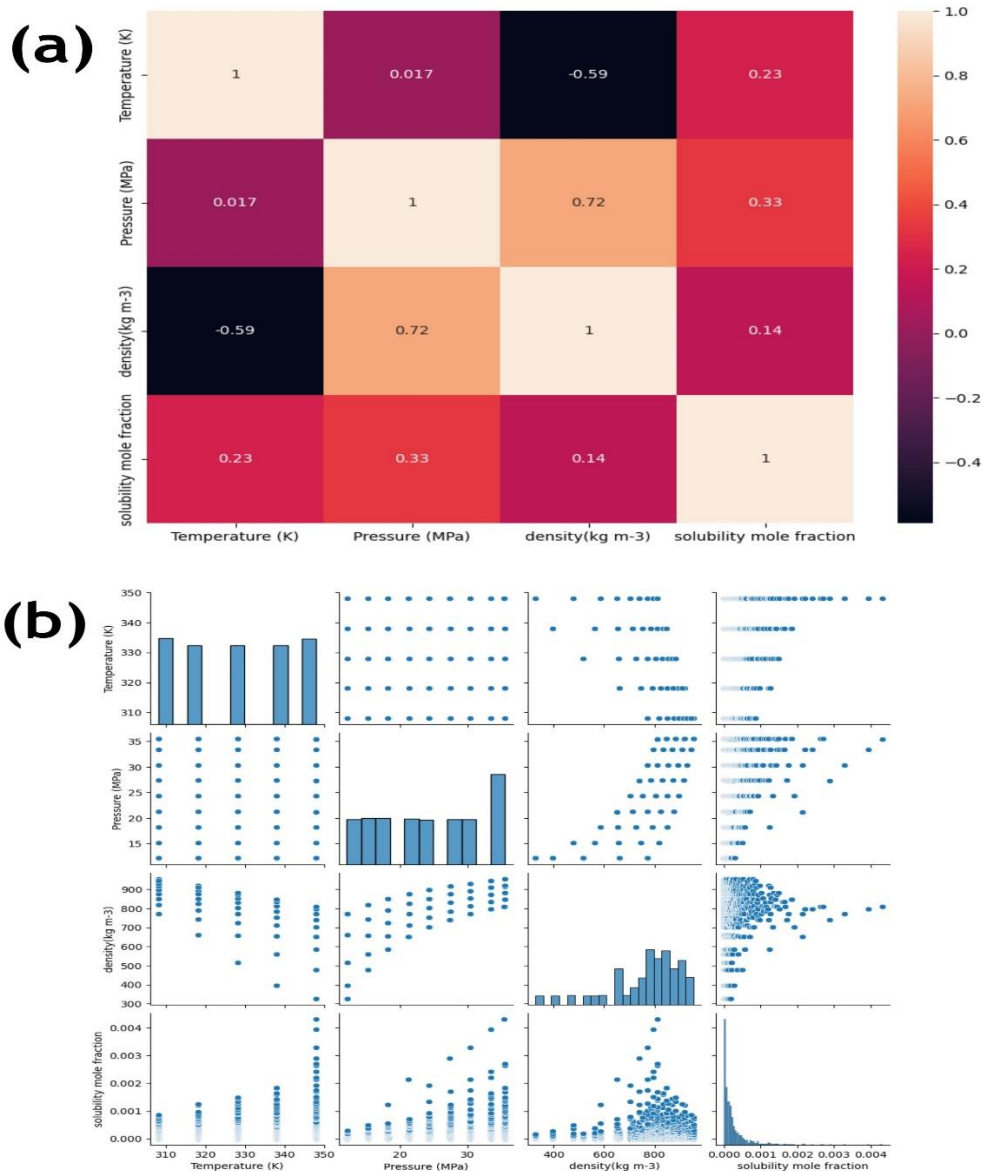
$$127 Data_{i,4} = \begin{bmatrix} T_{1,1} & P_{1,2} & D_{1,3} & y_{1,4} \\ \vdots & \vdots & \vdots & \vdots \\ T_{i,1} & P_{i,2} & D_{i,3} & y_{i,4} \end{bmatrix} \quad (1)$$

128 Where T is temperature in Kelvin, P is pressure in Mpa, D is density in Kg/m3 and y is solubility  
 129 mole fraction of the solute in the reaction mix. The index ‘i’, runs over the entire column of a  
 130 single feature. This is the first input data matrix required and is parsed by the scripts via the  
 131 Input\_Data.xlsx file.



132

133 **Fig. 1** Flow chart illustrating a single iteration by the parameter estimation, 3D visualization  
 134 and Predictive modeling program scripts



135

136 **Fig. 2** (a) Heat Map plot of correlation values of input parameters (Temperature, Pressure,  
 137 Density and Solute Mole fraction). (b) Parameter pair plot of data points including all  
 138 combinations of input parameters for illustrating patterns present among variable pairs  
 139

140 The second (required) matrix is comprised of the terms of the input density based semi  
 141 empirical equations. For illustration, consider a simple four parameter (however, users can input  
 142 any number of terms) linear model equation and its basic generalization,

143  $\ln(y) = A + B[T] + C[P] + D[\rho] \equiv Y = p_1[Term1] + p_2[Term2] + p_3[Term3] + p_4[Term4]$  (2)

144 Where, A, B, C, D corresponds to p1, p2, p3, p4 and are the parameter coefficients or estimands  
 145 of the DBSE model equation given above (however, users can input any number of terms). Let

146 these parameter coefficients be grouped into vector ‘P’. Let the terms of the model [term1,  
 147 term2, term3, term4] be grouped into a vector named as ‘Terms’. For the estimation of the  
 148 model coefficients in [P] and for obtaining parameter estimates  $\hat{p}$ , the terms of the sampled  
 149 DBSE model equations are input into respective cells of rows particular to each model equation  
 150 in a separate file (Models\_Equations.xlsx). These are the two input matrices required by the  
 151 MATLAB based parameter estimation script and the visualization script. A toy input data  
 152 sample containing 1000 experiments along with a sample of ten randomly selected,  
 153 semiempirical equations have been used for producing the output present in this article. The  
 154 possible modification path traversed by the data in a single iteration is illustrated (Fig. 1). Also,  
 155 the Input data is initially analyzed using basic statistical metrics in the Jupyter Notebook and  
 156 the outputs (Correlation heat map and parameter pair plot) are depicted (Fig. 2 a, b). Refer to  
 157 the user guide (given in the repository) for information on using these program scripts for  
 158 custom data and model equations (existing/newly proposed). The user guide also provides  
 159 information regarding the preselection of the base model along with the descriptions of the  
 160 randomly sampled model equations present in the unmodified file (Models\_Equations.xlsx).

161

### 162 *Parameter Estimation: Ordinary Least Squares Method*

163

164 Estimation of parameter coefficients represented in the vector P is performed using the method  
 165 of Ordinary Least Squares Parameter Estimation (Dismuke and C R Lindrooth 2006) in the  
 166 MATLAB program script (DBSE\_OLS\_Estimation.m). A concise development of the  
 167 implemented algorithm is presented. Consider a representation of a DBSE model equation in  
 168 the form of the classical linear regression model,

$$169 \quad Y_{i,1} = [\text{Terms}]_{i,k}[P] + \varepsilon_{i,1} \quad (3)$$

170 Let the assumptions, about the error in the models be, errors are additive, uncorrelated, has zero  
 171 mean and has constant variance.

172 Also,

$$173 \quad E(\varepsilon\varepsilon^T) = \sigma^2 I_i \quad (4)$$

174 Where  $\varepsilon$  is the residual vector and  $\sigma^2$  is the variance of the residual. Further, let the data  
 175 substituted, matrix of terms ‘Terms’ be represented for brevity as X and let Y be the vector of  
 176 natural logarithm of solubility mole fraction values. Then the ordinary least squares estimator  
 177  $\hat{p}$  is given by,

$$178 \quad \hat{p} = [X^T X]^{-1} X^T Y \quad (5)$$

179 The vector of residuals  $\varepsilon$  is given by,

180  $\varepsilon = Y - X\hat{p}$  (6)

181 The confidence intervals (bounds) of the estimates are computed at 95% confidence level.  
 182 Further, model selection is iteratively performed using an F-Statistic score (Belitser et al. 2011)  
 183 for each model equation relative to a preselected base model (This is input in the first row of  
 184 the Models\_Equations.xlsx file). Let the residual sum of squares for the DBSE model of a  
 185 particular iteration and the same for base model be,

186  $R_{ols}^{model} = \varepsilon_{ols}^T \varepsilon$   $R_{ols}^{base} = \varepsilon_{base}^T \varepsilon$  (7)

187 Then the equation for an F-score metric-based model selection is,

188 
$$\frac{\left( R_{ols}^{base} - R_{ols}^{model} \right) / (n_{p,0} - n_{p,base})}{R_{ols}^{model} / (n - n_{p,0})} > F_{(n_{p,0} - n_{p,base}), (n - n_{p,0})}^{0.05}$$
 (8)

189 Where  $n_{p,0}$  is the number of parameters in the current iteration and  $n$  is the number of data points  
 190 (experiments) in the parsed input data and  $n_{p,base}$  is the number of parameters in the base model.  
 191 In the data driven paradigm where modeling is focused on fitting a specific sample of empirical  
 192 data, this automated selection procedure is beneficial for decimating lower quality equations  
 193 and for identifying the most contextually appropriate one(s). Further, error metrics namely,  
 194 mean squared error (MSE), Root Mean Squared Error (RMSE), Mean Absolute error (MAE)  
 195 and Percentage Absolute Average Relative Deviation (% AARD) were computed between  
 196 experimental and predicted solubility using the expressions,

197  $Mean\ Squared\ Error = \frac{1}{n} \sum_{i=1}^n (\ln(y)_i^{pred} - \ln(y)_i^{exp})^2$  (9)

198  $Root\ Mean\ Squared\ Error = \sqrt{\frac{1}{n} \sum_{i=1}^n (\ln(y)_i^{pred} - \ln(y)_i^{exp})^2}$  (10)

199  $Mean\ Absolute\ Error = \frac{1}{n} \sum_{i=1}^n |(\ln(y)_i^{pred} - \ln(y)_i^{exp})|$  (11)

200  $\%AARD = \frac{100}{n} \sum_{i=1}^n \frac{|\ln(y)_i^{pred} - \ln(y)_i^{exp}|}{\ln(y)_i^{exp}}$  (12)

201 Error metrics have been computed using natural logarithm of solubility mole fraction values  
 202 for predictions after parameter estimation and actual solubility mole fraction values have been  
 203 used for predictions from predictive modeling.

204

205 ***Visualization of Phase Behaviour Projected by DBSE model Equations:***

206

207 Visualization of Phase behavior using three dimensional surfaces of the input DBSE model  
 208 equation is also implemented using MATLAB. The MATLAB script (DBSE\_3D\_Visualizer.m),

209 requires, model equations and empirical data (Input\_Data.xlsx and Models\_Equations.xlsx)  
210 along with the estimates (Parameter\_Predictions\_Results.xlsx) and iteratively plots three  
211 dimensional surfaces of the model equations using finitely spaced grid points of the parameters  
212 present in the particular DBSE model equation in the iteration.

213 Three surfaces are plotted by this script namely, Pressure-Temperature-Solute mole  
214 fraction, Density-Pressure-Solute mole fraction and, Density-Temperature-Solute mole  
215 fraction. Standard, inbuilt commands from MATLAB are used for plotting the surfaces for all  
216 of the input DBSE model equations. The output images are also in the standard interactive  
217 MATLAB plot window which allows for altering values of axes to obtain surfaces (Rovenski  
218 2010). Notedly, empirical data is used by this script only for finalizing extreme values of the  
219 grid points used for plotting these surfaces. Therefore, the surfaces plotted by this script  
220 illustrate phase behavior and vapor liquid equilibrium data projected by the specific DBSE  
221 model equation and these surfaces are not influenced by the pattern prevalent in the input  
222 empirical data. Finally, this script exports all three surfaces plotted for a DBSE model equation  
223 as subplots in a single image (.jpg) format.

224

225 ***Prediction of Solute Solubility: Machine Learning Algorithms***

226

227 Three Supervised Machine learning algorithms have been implemented using the Python  
228 module, Sklearn (Pedregosa et al. 2011) in a single Jupyter notebook  
229 (DBSE\_Predictive\_Modeling.ipynb) (Menke 2020). This Notebook, using input empirical data,  
230 in a single run, implements the Multilayer perceptron, K-nearest Neighbours regression and  
231 Support Vector regression algorithms before performing detailed and comparative analysis on  
232 the predictions and results. Standardized metrics are used for performing validation and analysis  
233 of results. Numpy (Oliphant 2006), Openpyxl, Pandas (W McKinney 2011), Matplotlib (Hunter  
234 2007) are among the python packages used for implementing these algorithms. This script  
235 requires empirical data (experiments in rows complete with Pressure, Temperature, Density and  
236 the resultant, solute mole fraction) characteristic to density based semi empirical model  
237 equations. Also, the input parameter space is not exhaustive and can incorporate additional  
238 parameters based on preference. Descriptions of the implemented algorithms and their tuneable  
239 hyperparameters are provided in the subsequent paragraphs.

240

241

242

## Multilayer Perceptron Regression [MLP]

243

244 Multilayer Perceptron [MLP] is a fully connected class of feed forward artificial neural  
245 networks classified as a supervised machine learning algorithm. This framework consists of  
246 updatable, weight assigned nodes called neurons that are sorted into three types of fully  
247 connected layers namely, input layer, hidden layer(s) and an output layer. During the training  
248 of a single instance (experiment), parameter (feature) information is fed into the input layer  
249 which is then transmitted to the next hidden layer(s) where activation function(s) modify this  
250 information for final modification in the output layer. The output layer, using an activation  
251 function, modifies the received information and provides data output. This output is the  
252 prediction value of the algorithm. Information modification during training (learning) results in  
253 the updation of the initialized weights (associated with neurons and connections) from the  
254 previous learning iteration (Murtagh 1991). In MLP, for obtaining accurate and precise output  
255 (solute solubility mole fraction), hyperparameter search space for size of hidden layer, neurons,  
256 activation functions, learning rate, data split ratio, solver, alpha value etc can be easily  
257 optimized in the notebook based on preference and data. Theoretical explanation and  
258 development of the MLP algorithm can be obtained in literature elsewhere (Schilling et al.  
259 2015). The results and analysis from this program code are finally saved (MI\_Results.xlsx).

260

261

## K-Nearest Neighbours Regression [KNN]

262

263 K- Nearest Neighbours algorithm is a non-parametric, supervised machine learning algorithm.  
264 For regression problems, the algorithm learns to predict the target class value based on the k  
265 closest training examples (instances or experiments) in the input data. The model during  
266 learning (training), performs search in the data pattern space for the closest number of training  
267 instances. The results from this search which are the closest ‘k’ number of training instances  
268 (neighbours), are averaged to obtain the prediction value (solute solubility mole fraction) during  
269 testing (Kramer 2013). The adjustable/tuneable hyperparameters for this algorithm is the ‘k’  
270 value (sampling metric) and the distance (closeness) measurement metric (Cunningham and  
271 Delany 2022). Here, Euclidean distances are calculated to measure closeness for the  
272 preassigned k value which is used to obtain a detailed, comparative, analysis of the prediction  
273 which also is saved (MI\_Results.xlsx).

274

275

## Support Vector Regression [SVR]

276

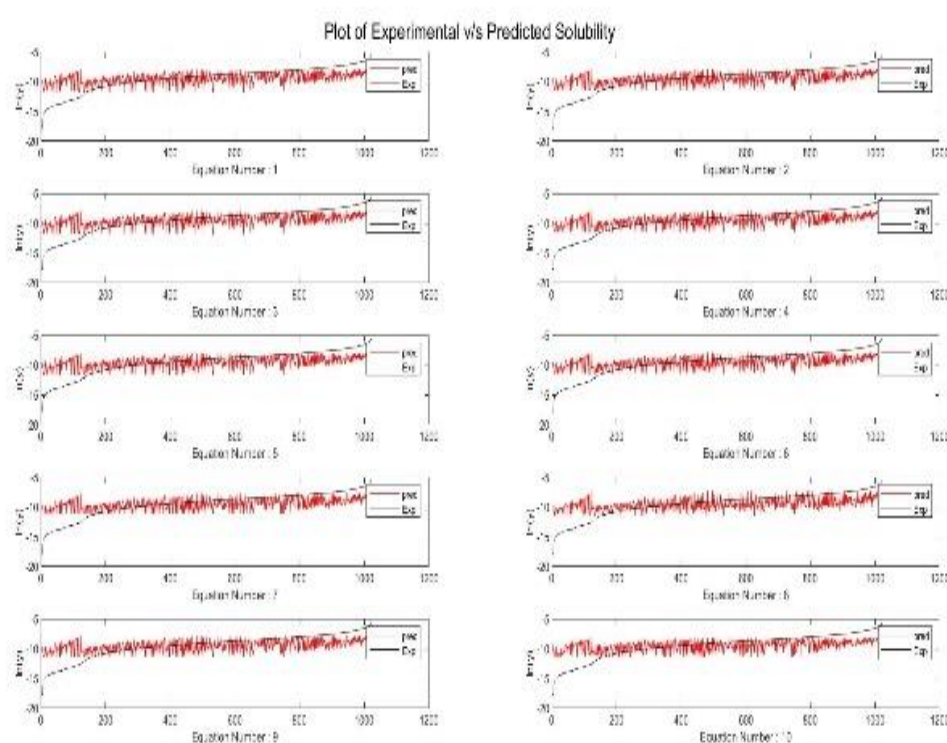
277 The support vector regression algorithm is a class of support vector machine algorithm and is  
 278 also a supervised machine learning algorithm. In fewer sentences, support vector regression  
 279 algorithm, using a kernel function, tries to map the input parameter variable data to a feature  
 280 space (usually of higher dimension) and with the aim of minimizing prediction error, tries to  
 281 find a hyperplane in this feature (parameter) space that maximizes the distance margin between  
 282 this plane and the closest data points. Theoretical development of the SVR technique and the  
 283 mechanism behind its prediction capabilities can be obtained in detail here (Smola and  
 284 Schölkopf 2004). The tuneable hyperparameters here are the kernel function, gamma value and  
 285 the test-train data split ratio. Scaling of the parameter data has not been implemented for SVR  
 286 as the pattern present in the parameter space is highly relevant for accurate prediction  
 287 (Tsirikoglou et al. 2017). The jupyter notebook, after implementing support vector regression,  
 288 separately provides results which also is saved (MI\_Results.xlsx).

289

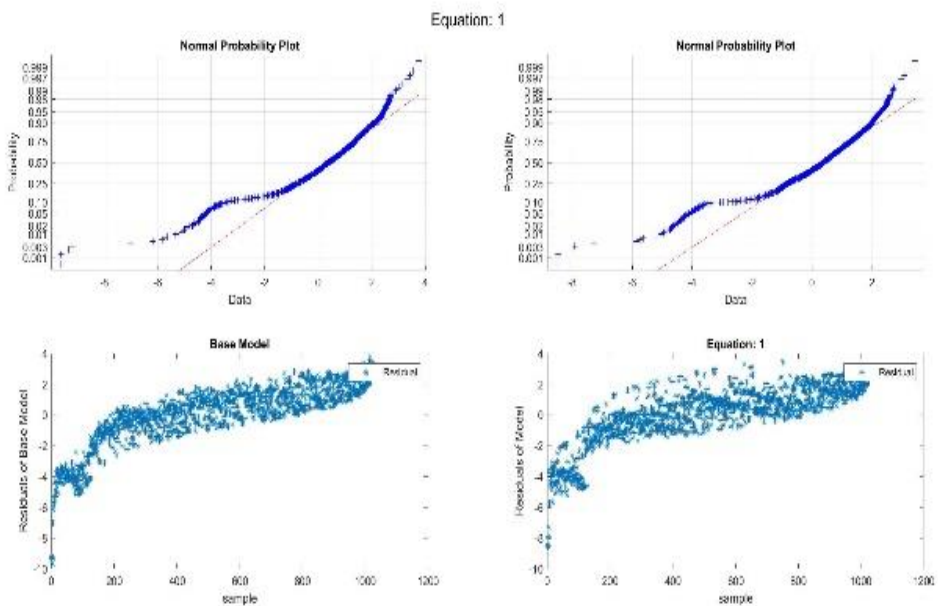
## Results and discussion

290

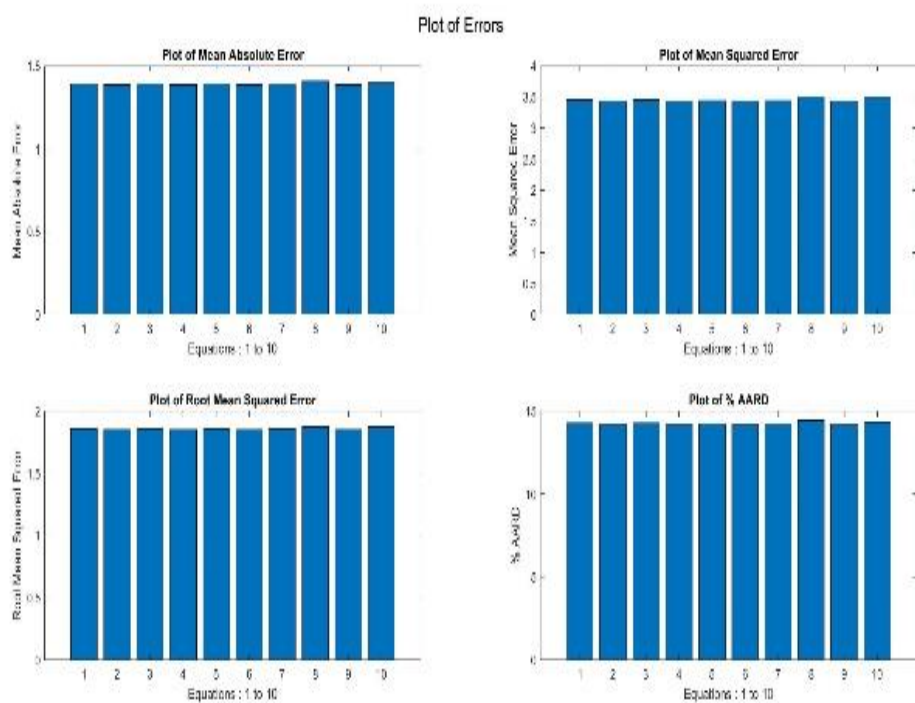
### *Parameter Estimation: Ordinary Least Squares Method*

**(a)**

(b)



(c)



291

292 **Fig. 3** Standard output (enlarged) for the model equation(s) being iterated from the MATLAB  
 293 based parameter estimation script. (a) Plot of Experimental (black) v/s Predicted (red) values  
 294 of the natural logarithm values of solute solubility molefraction. (b) Plot containing normality  
 295 plots and residual plots for base model equation of choice and the model equation being iterated.  
 296 (c) Bar plots pertaining to error metrics for all input equations.

297

298 As previously derived, A customized Ordinary least squares estimation method has been  
299 implemented to obtain parameter estimates of model equation constants along with confidence  
300 intervals in a ‘one model equation at a time’ iterative rule fashion. This ensures that the  
301 parameter (model coefficients) estimates are from a standardized and popularly used method  
302 used on all model equations in the batch sample (input using an .xlsx file). Confidence intervals  
303 (upper and lower bounds) are estimated for each estimate at 95 percent confidence.  
304 Conveniently, the results are saved and exported to retrievable file formats. The pictorial output  
305 from this script is shown in (Fig. 3 a – c). Natural logarithm values of solute solubility mole  
306 fractions are plotted against number of experiments for both empirical data and predictions  
307 made using the estimates (model constants) and state variables (Pressure, temperature and  
308 Density) associated with the model equations. Normality plots and residuals of the base model  
309 and the model equation (being iteratively estimated) are also charted for ascertaining the nature  
310 of the data. The normality and residual plots are shown (Fig. 3b). Normality plots reaffirm the  
311 considered assumptions about the residuals while estimating parameter coefficients (Model  
312 constants). This step makes sure the estimates are contingent with the assumptions made  
313 regarding the data and by extension, also the residuals. In the Fig. 3 b above, the data appear to  
314 lie on the line of reference demonstrating the degree of normality present in the sample data.  
315 Unfortunately, the large amount of data (from the toy data sample) in the shown residuals plot  
316 indicate a pattern and masks the randomly distributed points in the region of interest. This  
317 region of interest corresponds to the operating conditions where solute solubility is supposedly  
318 maximum/optimum (window of maximum solubility). However, this also will change when  
319 different empirical data is used. Scores computed from F Distribution, provide clear, statistical  
320 comparison between the model equation being iteratively estimated and the base model  
321 equation of choice (Input in the first row in the Models\_Equations.xlsx file). Additionally,  
322 excellent inference can be made based on published literature regarding the estimates and  
323 selection output produced by this program (Garlapati and Madras 2010; Reddy and Madras  
324 2011; Bian et al. 2016; Alwi and Garlapati 2021b). The pictorial illustration indicates the  
325 plotting constraints (maximum number of subplots in the image output) associated with the  
326 presented code and it is encouraged to consider this factor while sampling model equations.  
327 Plotting natural logarithm values of the predicted data against actual solute solubility mole  
328 fraction values of the predicted data (from model equations), provides clear distinction and  
329 higher resolution of model fit and deviation from empirical data. Errors and residuals are also  
330 calculated using natural logarithm values for this important reason. In reality, based on the toy  
331 sample empirical data, the error metrics and residuals appear to be significantly (desirably) low

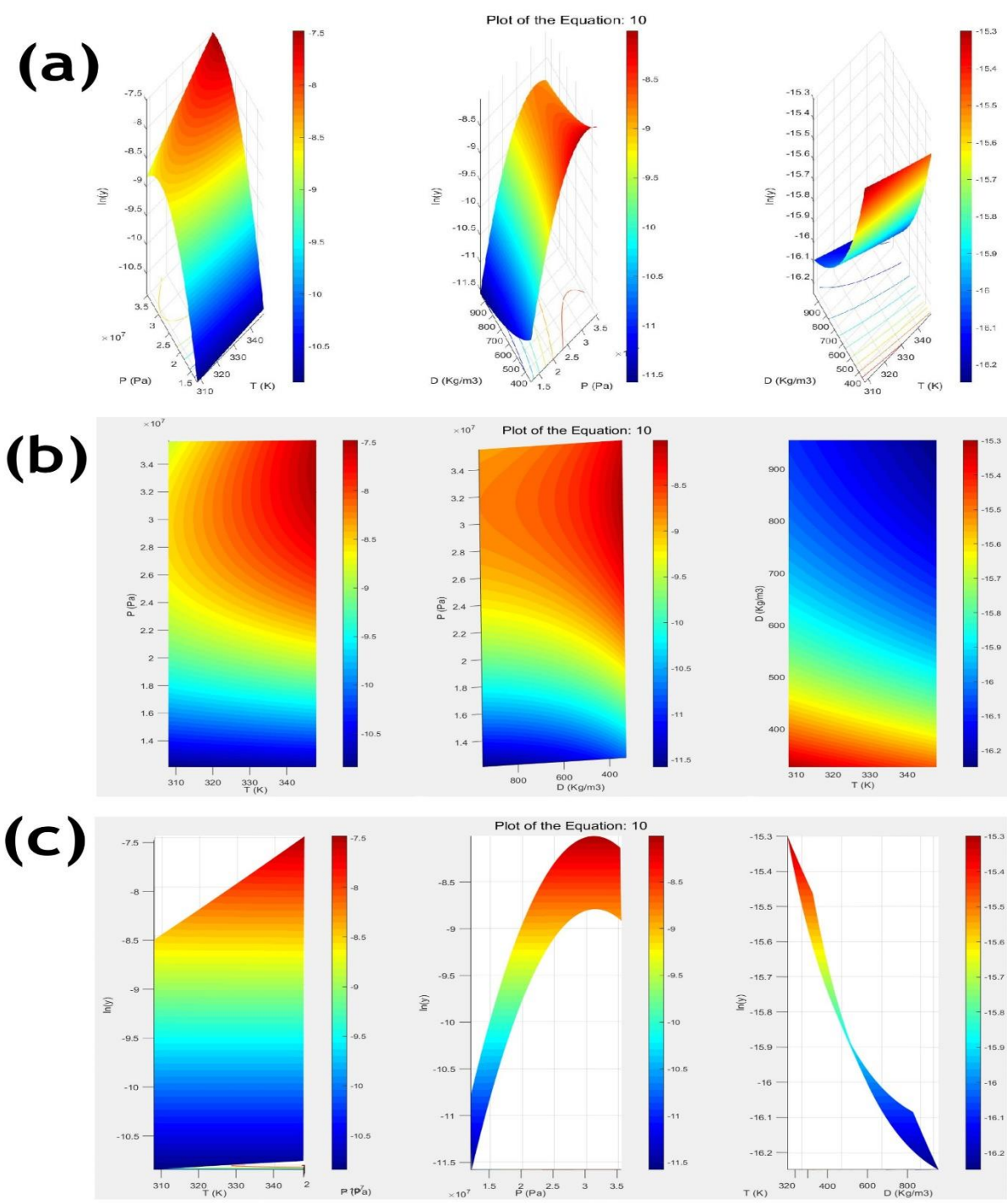
when actual solubility values are used as opposed to their natural logarithm values. Mean squared error (MSE), Root Mean Squared Error (RMSE), Mean Absolute error (MAE) and Percentage Absolute Average Relative Deviation (% AARD) values are computed using Eq. (9)-(12), plotted and presented in the form of bar graphs in a single image format (Fig. 3 c). Errors of all model equations appear to only slightly differ indicating superior quality of the sampled toy data. However, as previously mentioned, this too will differ for other empirical data. Due to constraints for assessing and visualizing higher numbers of equations, sampling (ten to fifteen equations) and selection of model equations (for achieving column rank) must be of higher quality. However, the provided code for batch estimation (DBSE\_OLS\_Estimation\_Batch.m), has full capability to estimate as many as a hundred DBSE model equations in a single implementation.

In summary, this program script provides parameter estimates of model(s) coefficients along with their confidence regions (intervals). Further, the model selection and identification routine is also favorable for comparative assessment and selection of the best performing model equation all of which are then exported to popular file formats.

347

348

**Visualization of Phase Behavior projected by DBSE Model Equations:**



349

350 **Fig. 4** Three dimensional surfaces of  $\ln(y)$ -P-T,  $\ln(y)$ -D-P,  $\ln(y)$ -D-T. (a) This plot is the only  
 351 standard output produced by the MATLAB based visualization script. (b) Two dimensional,  
 352 color coded contour plot of P-T, P-D, D-T obtained from the same MATLAB interactive plot  
 353 window. The projections for these plots are visible on the respective 3D surface (a). (c) Two  
 354 dimensional, color coded contour plot of  $\ln(y)$ -T,  $\ln(y)$ -D,  $\ln(y)$ -D obtained from the MATLAB  
 355 interactive plot window.

356 The three-dimensional surfaces of the P-T-D state variables and the natural logarithm values of  
 357 solute solubility mole fraction obtained from this script for visualization is illustrated in Fig. 4  
 358 a – c. The interactive nature of the MATLAB surface plot window and the ease with which axes  
 359 values of the plotted surface can be altered makes the obtained pictorial output invaluable for  
 360 evaluating the phase equilibria characteristic to the respective DBSE model equation. Fig. 4 a  
 361 shows a grab of the three surfaces [P-T- $\ln(y)$ , P-D- $\ln(y)$ , T-D- $\ln(y)$ ] arranged as subplots from  
 362 a single interactive (image) window output. As previously mentioned, Grabs of two-  
 363 dimensional plots (Fig. 4 b – c) can be obtained from these surfaces by independently altering  
 364 the axes values of the surfaces in the interactive MATLAB plot window. The surfaces are  
 365 primarily color coded to indicate the gradient in solute solubility. Projections of these surfaces  
 366 manifest as grid lines (phase curves of  $\ln(y)$ ) on the axes planes. These plots indicate the major  
 367 and minute differences in the projected phase behavior put forth by the model equations.  
 368 Conveniently, even small or minute variations in a combinatorial pool of model equation  
 369 designs (derived from a parent equation) manifests acutely in the shape and color gradient of  
 370 the corresponding surface plots (Goos et al. 2011; Yamini and Moradi 2011; Cockrell et al.  
 371 2021). Further, literature (Schneider 1978; Mouahid et al. 2022) can be referred to make  
 372 accurate inferences regarding model specific phase behavior from these surfaces and  
 373 projections. However, a probable/possible approach (from the users' perspective) for gaining  
 374 satisfactory information from these surfaces (3D), its derivative plots and plane projections  
 375 (2D) is provided below.

376 Consider a set of model coefficient parameter estimates, from a DBSE model equation,  
 377 derived from empirical data from a (sufficiently) well modelled super/sub critical fluid  
 378 extraction process (for example, coffee or tea decaffeination) pertaining to a ternary system of  
 379 CO<sub>2</sub>/H<sub>2</sub>O solvent, Co-solvent (Ethanol or methanol) and solute (This ground truth data is  
 380 subject to availability and procurement by the user and is not provided here in/with this article).  
 381 Let this set of obtained estimates (which are highly process centric and equation specific) be  
 382 then used to plot the 3D surfaces and derivative plots (from this script). Naturally, due to the  
 383 process being sufficiently well modelled (as previously assumed), knowledge regarding the  
 384 projected Phase diagrams, vapor-liquid equilibrium behavior, maximum/optimal/desirable  
 385 solubility window and equilibrium points and planes is readily available, importantly reliable  
 386 and trustworthy for these estimates (ground truth), plots and the associated empirical data. Let  
 387 this information (again, not provided here with this article) be the ground truth and basis for  
 388 performing further comparative analysis using the MATLAB based plotting and visualization  
 389 script presented here in this article. Then the surfaces and 2D projections obtained by

390 implementing this visualization script for the same empirical data (and the model coefficient  
 391 estimates) for a batch of DBSE model equations (existing/newly developed) can now be used  
 392 to evaluate and glean information regarding the optimal window and other important associated  
 393 attributes like the upper and lower critical end points, planes and edges associated with latency  
 394 and the triple point. Further, vapor pressure curves and the data characteristic to the components  
 395 (pure and mixture) in the ternary system can be identified and compared to this ground truth.

396 Generally, the qualitative and quantitative data regarding the latency, miscibility,  
 397 compression, crystallizability of the components in the reaction mix can be obtained from these  
 398 surfaces. Further, the identified solid-liquid-gas lines (by using cursor on the surface and  
 399 comparing point coordinates) describing boundaries of latency (or miscibility) projected on the  
 400 surface specific to the DBSE model equation(s) can also be compared to this (empirical) truth  
 401 and the error values quantify deviation and subtle / major differences. Similarly, values of slope  
 402 differentials ( $dP/dT$ ,  $dT/dD$  and  $dP/dD$ ) are easily computed from the surfaces for these  
 403 equations. The computed slope values could be used to identify upper and lower crossover  
 404 pressures bordering the retrograde solubility region in the phase diagrams for explaining /  
 405 utilizing retrograde solubility interference (Foster et al. 1991; Esmaeilzadeh and Goodarznia  
 406 2005; Kalikin et al. 2021). This is useful for screening newly designed DBSE model equations  
 407 for the maximum/optimal solubility window and the basis of which can further be used for  
 408 iteratively optimizing the optimal solubility window (by region specific selection), redesigning  
 409 customized, newer and efficient model equation alternatives. Overall, This Comparative  
 410 evaluation based on this ground truth is useful for selecting equations that project phase  
 411 behaviour with higher resolution and accuracy within the newly estimated/optimized optimal  
 412 solubility window. The Phase behavior projected from this particular newly selected equation  
 413 will now prove to be more beneficial for decision making and dynamic process optimization  
 414 (better than the present ground truth data).

415 Often, In Pilot / Production scale equipment, optimization is focused on Cost  
 416 effectiveness and dynamic feasibility factors (that influence cost effectiveness) including, but  
 417 not limited to, Process duration/Residence time, Resource consumption/availability, Climate  
 418 change/Ambient physical conditions, Hazard/Risk propensity among others. In such scenarios,  
 419 optimal solubility windows (based on current feasibility thresholds) can be estimated/optimized  
 420 (using this script) and implemented for large scale extraction. Conversely, Phase and VLE data  
 421 from the optimized surfaces derived from Model equations that are specifically designed (using  
 422 this work) for a particular process can potentially inform future decisions and process  
 423 trajectories for meeting optimal feasibility goals. Note that the maximum solubility window

424 (Not the optimal solubility window) depicted in Figure 4(b) is predicted and shown to lie around  
 425 the red regions (between 320K-340K and 30-32 MPa) by the tenth model equation (from the  
 426 same randomly mined sample of ten input equations). As pictorially shown, and explained, the  
 427 optimal solubility window is largely exploratory, process centric and will differ for a different  
 428 sample of equations for the same data (empirical ground truth) or other obvious differences in  
 429 physical parameters (residence time and quantity of reaction mix etc). To summarize, the plots  
 430 provide satisfactory, quantitative and qualitative knowledge regarding the phase behavior and  
 431 equilibria characteristic to the equations being studied, using this MATLAB based plotting and  
 432 visualization script.

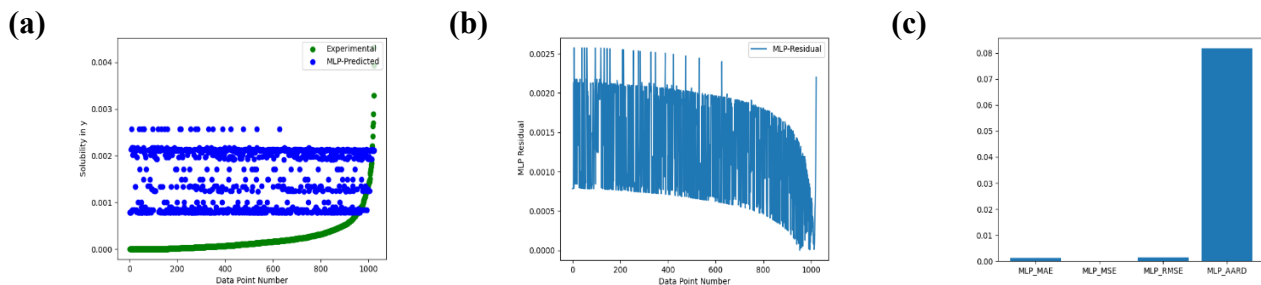
433

#### 434 ***Prediction of Solute Solubility: Machine Learning Algorithms***

435

436 Multilayer Perceptron regression (MLP), K-Nearest Neighbours regression (KNN) and Support  
 437 Vector Regression (SVR) algorithms have been implemented using ‘sklearn’ package in python  
 438 in a single jupyter notebook. A toy data sample of 1000 randomly mined experiments are used  
 439 to illustrate the working of this jupyter notebook. The input parameters present in the toy data  
 440 sample are Temperature, Pressure and Density. The target / output / dependent variable is the  
 441 Solute solubility mole fraction. Additional parameters can be easily incorporated into the data  
 442 sample by simply concatenating them as columns after the Density data column in the input  
 443 data (Input\_Data.xlsx). The notebook initially provides description of the data using basic  
 444 statistical metrics (count, mean, standard deviation, minimum and maximum value),  
 445 Correlation values between the parameters and output, Heat map of correlation values and a  
 446 parameter pair plot for comparing the considered parameter pairs (combinations) on a chart.  
 447 These charts are shown in (Fig. 2 a – b). The results (graphs, errors and plots) and discussion  
 448 pertaining to each algorithm is provided in the subsequent paragraphs.

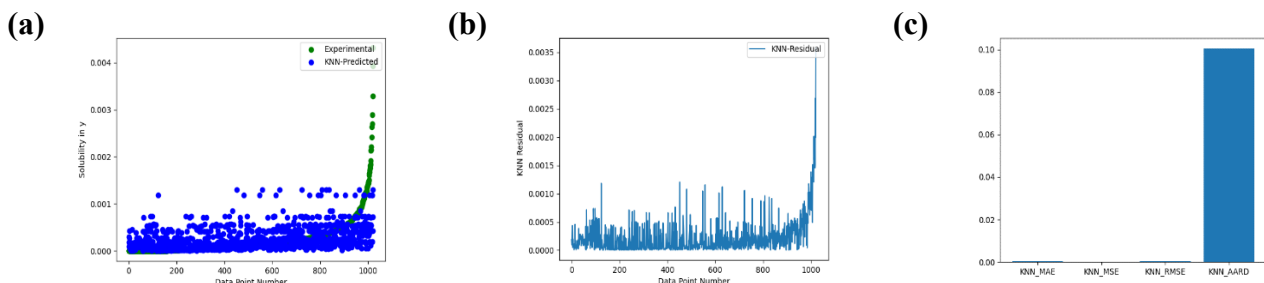
449



450

451 **Fig. 5** Standard output from the jupyter notebook about the predictions and analysis of the  
 452 Multilayer perceptron algorithm (a) Scatter Plot of Experimental (green) v/s Predicted (blue)  
 453 values of solute solubility molefraction from the Multilayer perceptron algorithm. (b) Plot of  
 454 residual values from the Multilayer perceptron algorithm. (c) Bar plot of error metrics of the  
 455 predictions from the Multilayer perceptron algorithm.

456 Multilayer Perceptron regression (MLP) is the first algorithm implemented in this  
 457 Jupyter notebook. Data scaling (preprocessing) is performed using the ‘MinMaxScaler’ routine  
 458 before further transformation of the data. The data is then split (preprocessing) using the test-  
 459 train-split routine. The results and the output obtained are illustrated in Fig. 5 a – c. Regression  
 460 model is built using the standard ‘MLPRegressor’ routine. Hyperparameter optimization / tuning  
 461 is performed using the ‘GridSearchCV’ routine for the MLP algorithm. As explained, the space  
 462 for grid search for the hyperparameters (Number of hidden layers, activation functions, solvers,  
 463 learning rate) has to be defined in the beginning of the notebook for hyperparameter  
 464 optimization. Further, 5-fold cross validation is performed based on negated values of root  
 465 mean square error as the model scoring metric. The program performs tuning and the  
 466 hyperparameters of the best model are then used to refit and obtain the prediction output  
 467 (Schilling et al. 2015). Error metrics for this algorithm are (output) plotted (Fig. 5 c) separately.  
 468



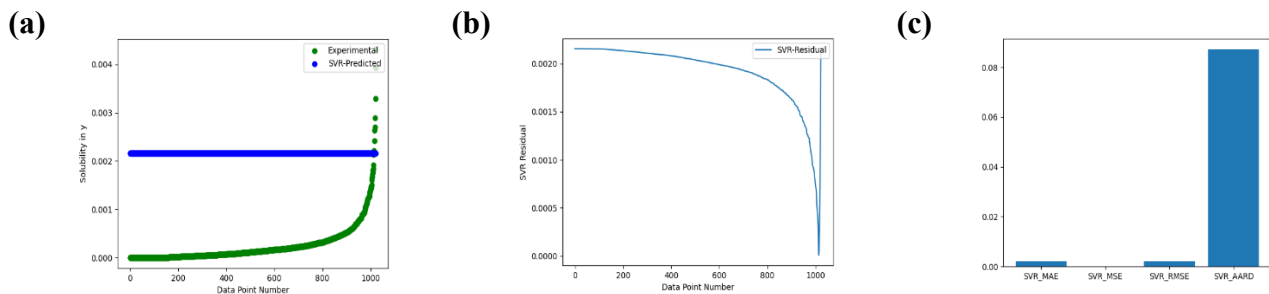
469

470 **Fig. 6** Standard output from the jupyter notebook about the predictions and analysis of the K-  
 471 Nearest Neighbours algorithm. (a) Scatter Plot of Experimental (green) v/s Predicted (blue)  
 472 values of solute solubility molefraction from the K- Nearest Neighbours algorithm. (b) Plot of  
 473 residual values from the K- Nearest Neighbours algorithm. (c) Bar plot of error metrics from  
 474 the K- Nearest Neighbours algorithm.

475 K-Nearest Neighbours regression (KNN) is implemented after MLP in the notebook.  
 476 As discussed, Data scaling was deemed unnecessary and has not been performed. However,  
 477 test train split is performed using the same routine as MLP. Further, The Hyperparameter K is  
 478 set to a random value of 3 for the toy data sample and can easily be changed / tuned based on

479 data and preference at the beginning of the notebook. Error metrics for the KNN algorithm is  
 480 plotted (Fig. 6 c) separately. Further insight regarding the model can be obtained from data,  
 481 hyperparameter optimization and previous literature (Soleimani Lashkenari and KhazaiePoul  
 482 2017).

483

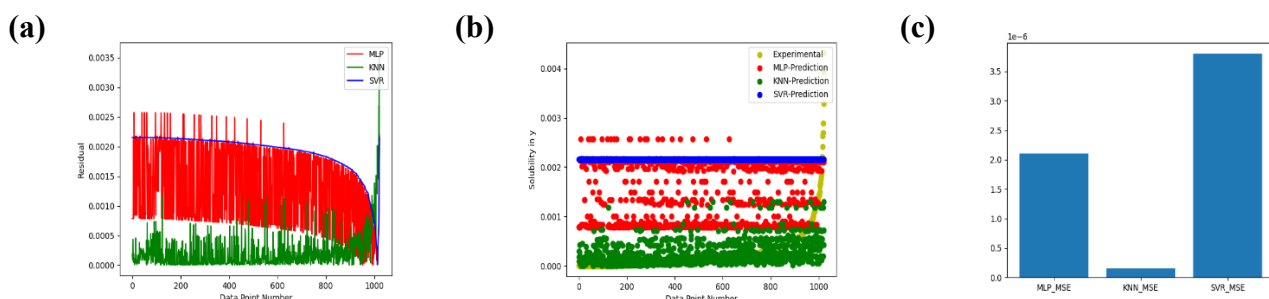


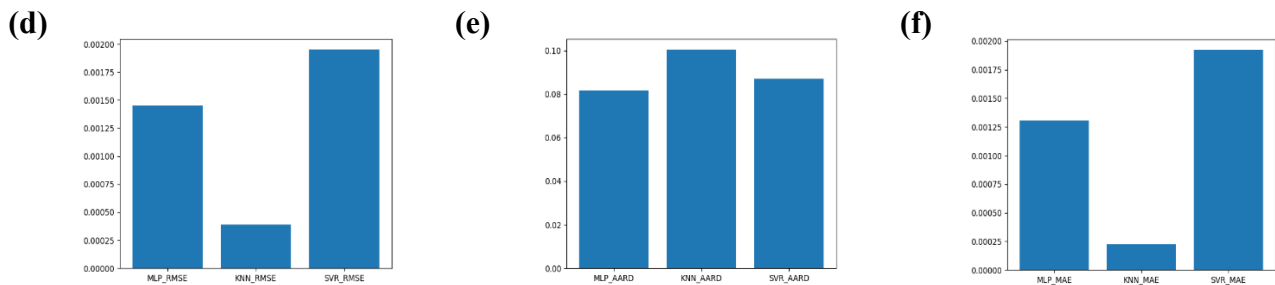
484

485 **Fig. 7** Standard output from the jupyter notebook about the predictions and analysis of the  
 486 Support Vector Regression algorithm. (a) Scatter Plot of Experimental (green) v/s Predicted  
 487 (blue) values of solute solubility molefraction from the Support Vector Regression algorithm.  
 488 (b) Plot of residual values from the Support Vector Regression algorithm. (c) Bar plot of error  
 489 metrics from the Support Vector Regression algorithm.

490 Support Vector Machine Regression (SVR) algorithm is implemented next in the  
 491 notebook. Like before, data scaling is not performed so as to preserve pattern in the input  
 492 parameter space. Data has been split for model training using the test – train split routine like  
 493 before and can be easily adjusted. The choice of Kernel function hyperparameter is also tuned  
 494 using ‘GridSearchCV’ and the grid search space can be modified for this at the beginning of  
 495 the notebook. Five-fold cross validation is performed based on the negated root mean squared  
 496 error scoring metric and the kernel function associated with the best scoring model is then used  
 497 to refit and obtain the predictions (Tsirikoglou et al. 2017). Error metrics for SVR, like before,  
 498 is also plotted (Fig. 7 c) separately.

499





500

501 **Fig. 8** Standard output from the jupyter notebook about the predictions and comparative  
 502 analysis of all three algorithms from each complete program run. (a) Combined plot of residual  
 503 values of all three machine learning algorithms (MLP, KNN, SVR) for comparison (b) Plot of  
 504 Prediction values of KNN and SVR algorithms with experimental solubility values. (c) Bar plot  
 505 of mean squared error values of all three machine learning algorithms (MLP, KNN, SVR) for  
 506 comparison. (d) Bar plot of root mean squared error values of all three machine learning  
 507 algorithms (MLP, KNN, SVR) for comparison. (e) Bar plot of percent absolute average relative  
 508 deviation values of all three machine learning algorithms (MLP, KNN, SVR) for comparison.  
 509 (f) Bar plot of mean absolute error values of all three machine learning algorithms (MLP, KNN,  
 510 SVR) for comparison.

511 Model fitting and prediction of all three algorithms (MLP, KNN and SVR) for the  
 512 sample data yielded results and the computed errors (MSE, RMSE, MAE and %AARD) are  
 513 plotted separately on bar plots (Fig. 8 c, d, e, f). The predictions v/s empirical data graph is also  
 514 plotted and exported by the notebook (Fig. 8 b). Likewise, residuals are also plotted for all three  
 515 algorithms (Fig. 8 a). Hyperparameter tuning for all three algorithms is implemented and other  
 516 intricate nuances (relative parameter importance, stacking of experiments based on specific  
 517 parameters/order) pertaining to the predictions can be easily made based on the best performing  
 518 algorithm and the input data (Feurer 2019). The parameter space, as previously explained, can  
 519 (only) be increased to explore and incorporate additional parameters like Residence time,  
 520 Mass/Volume of Raw Material, Viscosity of the Material, Melting point, Boiling Point, Total  
 521 polar surface area, Critical Temperature, Critical Pressure, Molecular Weight of solute,  
 522 percentage of co-solvent used, type of cosolvent (by scoring) etc. Therefore, Detailed  
 523 explanation regarding the obtained numerical output is unnecessary here since a toy data sample  
 524 with the standard (Temperature, Pressure and Density) parameters has been studied. The  
 525 notebook includes the best of the available plot commands and features (errors, functions, tables  
 526 etc) from standard python libraries for ease of use and assessment. The numerical data  
 527 predictions and analysis are also saved and exported to popular file formats (.xlsx). Importantly,

528 users are cautioned against the usage of this notebook for actual experimental purposes as it can  
529 be dangerous when used directly in a laboratory setting without proper consultation and  
530 reasoning. The provided notebook is an efficient exploratory tool for data analysis and is very  
531 useful for theoretical research, modeling (fitting), understanding and comparison. Overall, This  
532 Jupyter notebook is a state-of-the-art predictive modeling and analysis tool using standard  
533 Machine learning algorithms for obtaining prediction values of solute solubility mole fraction  
534 from input parameter data.

535

536

## Conclusions

537

538 This work describes software program scripts and presents their workflow as a comprehensive,  
539 state of the art parameter estimation and predictive modeling tool for evaluating density based  
540 semi empirical models (equations) and its associated data. Parameter estimation has been  
541 implemented in a MATLAB based script using a customized version of the popular Ordinary  
542 least squares estimation method. Further in this work, Visualization of phase behaviours  
543 projected by preselected (sampled) model equations using a MATLAB based script has been  
544 described. This visualization script produces three-dimensional surface plots in interactive  
545 MATLAB windows based on the parameter estimates (computed from ordinary least squares  
546 estimation). An approach for gleaning theoretical information regarding phase behaviour using  
547 the surface plots is provided. Importantly, even subtle variations among model equations  
548 acutely manifests in the shapes and color gradients of the projected surface plots and this makes  
549 designing newer, robust, data specific/generalized equations easier. Standardized error and  
550 scoring metrics have been computed at each appropriate stage in the workflow and is presented  
551 in the form of plot illustrations. Importantly, the maximum solubility window is predicted to lie  
552 somewhere around the red regions (probably between 320K-340K and 30-32 MPa) by the tenth  
553 model equation (and is predicted for all the remaining input equations). The visualization  
554 program is stand alone in that it fully functions when parameter estimates and parameter  
555 boundaries for input equations are externally sourced. A Python based programming script is  
556 also presented for predictive modeling of the associated input empirical data using three  
557 Machine learning algorithms. Also, this notebook has been written to accommodate ‘n’ number  
558 of other variables for improving the accuracy of the solute solubility predictions. This allows  
559 users with diverse forms of data to easily make predictions, interpretations and reach  
560 scientifically sound conclusions about the maximum/optimal solubility window. Further, user  
561 defined hyperparameter tuning has been implemented for all three algorithms and has not been

562 entirely focused towards fitting the toy data sample (However, the presented error metrics are  
 563 desirably low). Therefore, it is strongly advised to use these program scripts for theoretical and  
 564 academic purposes since these scripts are under continuous development, refinement and  
 565 modification. The surfaces, plots and tables present in this article are the standard predictions  
 566 and analysis of outputs from these scripts based on a toy data and model equation(s) sample  
 567 (mined randomly from literature) and are not regarding any particular density based semi  
 568 empirical equation or published data. Hence, again, strong caution is advised against the usage  
 569 of any aspect of this work directly in an experimental setting without appropriate supervision  
 570 or reasoning. Importantly, a properly worded guide is provided for using this repository. Future  
 571 goals include deploying and testing this work on a GUI, established datasets, on temporal  
 572 variation, similar computational tools, and DBSE model equations. In summary, this work  
 573 postures a first of its kind, efficient computational tool in the form of program scripts for  
 574 evaluating/designing Density based semi empirical equations associated with super/sub critical  
 575 extraction process and data.

576

577 **Data Availability.** The Software programs are available in a GitHub Repository here  
 578 <https://github.com/Srinidhi-hub/DBSE-Evaluator.git>. The software programs are also  
 579 accessible upon request from the author.

580

581 **Conflict of Interest.** The Author declares that there are no conflicts of interests with any entity,  
 582 institution or individual regarding this study. The author also declares that this study/work did  
 583 not receive any funding from any source.

584

585 **Acknowledgements.** The Author is grateful to Prof. Dr. Rudiyanto Gunawan (Graduate  
 586 Academic/Research Advisor during my Graduate studies), Lab members, Professors, and  
 587 Colleagues at UB-CBE.

588

**Author Biography:** Srinidhi received his Master's degree in Chemical Engineering from The State University of New York at Buffalo (University at Buffalo) (CeDiD: 22G6-XJHD-SOI8). Earlier, he received his Bachelor's degree in Biotechnology Engineering from M. S. Ramaiah Institute of Technology. His Academic Interests include Mathematical modeling of Chemical and Biological Processes.



589

590

**Symbols**

591

592 T

Temperature

K

593 P

Pressure

MPa

594 D

Density

Kg/m<sup>3</sup>

595 R

Residual Sum of Squares

596 y

Solute Solubility Mole Fraction

597

598 **Greek Letters**

599

600 ε

Error

601 σ

Standard Deviation

602 ρ

Density

Kg/m<sup>3</sup>

603

604

605

**References**

606

607 Alwi RS, Garlapati C (2021a) A new semi empirical model for the solubility of dyestuffs in  
 608 supercritical carbon dioxide. Chemical Papers 75:2585–2595.  
 609 <https://doi.org/10.1007/s11696-020-01482-x>

610 Alwi RS, Garlapati C (2021b) A new model and estimation of thermodynamic parameters for  
 611 the solubility of azobenzene and anthraquinone derivatives in supercritical carbon dioxide.  
 612 Chemical Papers 75:4589–4610. <https://doi.org/10.1007/s11696-021-01688-7>

613 Asgarpour Khansary M, Amiri F, Hosseini A, et al (2015) Representing solute solubility in  
 614 supercritical carbon dioxide: A novel empirical model. Chemical Engineering Research  
 615 and Design 93:355–365. <https://doi.org/10.1016/j.cherd.2014.05.004>

616 Bartle KD, Clifford AA, Jafar SA, Shilstone GF (1991) Solubilities of Solids and Liquids of  
 617 Low Volatility in Supercritical Carbon Dioxide. J Phys Chem Ref Data 20:713–756.  
 618 <https://doi.org/10.1063/1.555893>

619 Belitser S V., Martens EP, Pestman WR, et al (2011) Measuring balance and model selection  
 620 in propensity score methods. Pharmacoepidemiol Drug Saf 20:1115–1129.  
 621 <https://doi.org/10.1002/PDS.2188>

622 Bian XQ, Zhang Q, Du ZM, et al (2016) A five-parameter empirical model for correlating the  
 623 solubility of solid compounds in supercritical carbon dioxide. Fluid Phase Equilib 411:74–  
 624 80. <https://doi.org/10.1016/j.fluid.2015.12.017>

625 Butler KT, Davies DW, Cartwright H, et al (2018) Machine learning for molecular and  
 626 materials science. Nature 559:547–555. <https://doi.org/10.1038/s41586-018-0337-2>

627 Cockrell C, Brazhkin V V., Trachenko K (2021) Transition in the supercritical state of matter:  
 628 experimental evidence. Phys Rep. <https://doi.org/10.1016/j.physrep.2021.10.002>

629 Cunningham P, Delany SJ (2022) k-Nearest Neighbour Classifiers - A Tutorial. ACM Comput  
 630 Surv 54:1–25. <https://doi.org/10.1145/3459665>

- 631 Dismuke, C R Lindrooth (2006) Ordinary least squares :Methods and Designs for Outcomes  
 632 Research
- 633 Esmaeilzadeh F, Goodarznia I (2005) Supercritical Extraction of Phenanthrene in the Crossover  
 634 Region. *J Chem Eng Data* 50:49–51. <https://doi.org/10.1021/je049872x>
- 635 Feurer M (2019) Automated Machine Learning. Springer International Publishing, Cham
- 636 Foster NR, Gurdial GS, Yun JSL, et al (1991) Significance of the crossover pressure in solid-  
 637 supercritical fluid phase equilibria. *Ind Eng Chem Res* 30:1955–1964.  
 638 <https://doi.org/10.1021/ie00056a044>
- 639 Garlapati C, Madras G (2010) New empirical expressions to correlate solubilities of solids in  
 640 supercritical carbon dioxide. *Thermochim Acta* 500:123–127.  
 641 <https://doi.org/10.1016/j.tca.2009.12.004>
- 642 Goos E, Riedel U, Zhao L, Blum L (2011) Phase diagrams of CO<sub>2</sub> and CO<sub>2</sub>–N<sub>2</sub> gas mixtures  
 643 and their application in compression processes. *Energy Procedia* 4:3778–3785.  
 644 <https://doi.org/10.1016/j.egypro.2011.02.312>
- 645 Hawthorne SB (1990) ANALYTICAL-SCALE SUPERCRITICAL FLUID EXTRACTION.  
 646 *Anal Chem* 62:633A–642A. <https://doi.org/10.1021/ac00210a722>
- 647 Herrero M, Mendiola J, ... AC-J of C, 2010 undefined (2010) Supercritical fluid extraction:  
 648 Recent advances and applications. Elsevier 1217:2495–2511.  
 649 <https://doi.org/10.1016/j.chroma.2009.12.019>
- 650 Huang Z, Shi X, Jiang W (2012) Theoretical models for supercritical fluid extraction. *J  
 651 Chromatogr A* 1250:2–26. <https://doi.org/10.1016/j.chroma.2012.04.032>
- 652 Hunter JD (2007) Matplotlib: A 2D Graphics Environment. *Comput Sci Eng* 9:90–95.  
 653 <https://doi.org/10.1109/MCSE.2007.55>
- 654 Kalikin NN, Oparin RD, Kolesnikov AL, et al (2021) A crossover of the solid substances  
 655 solubility in supercritical fluids: What is it in fact? *J Mol Liq* 334:115997.  
 656 <https://doi.org/10.1016/J.MOLLIQ.2021.115997>
- 657 Khatib M El, de Jong WA (2020) ML4Chem: A Machine Learning Package for Chemistry and  
 658 Materials Science. arxiv.org. <https://doi.org/https://doi.org/10.48550/arXiv.2003.13388>
- 659 Knez Ž, Škerget M, KnezHrnčič M (2013) Principles of supercritical fluid extraction and  
 660 applications in the food, beverage and nutraceutical industries. In: Separation, Extraction  
 661 and Concentration Processes in the Food, Beverage and Nutraceutical Industries. Elsevier,  
 662 pp 3–38
- 663 Kramer O (2013) K-Nearest Neighbors. pp 13–23
- 664 Lakshmi K, Mahaboob B, Rajaiah M, Narayana C (2021) Ordinary least squares estimation of  
 665 parameters of linear model. *Journal of Mathematical and Computational Science* 11:2015–  
 666 2030. <https://doi.org/10.28919/jmcs/5454>
- 667 Matlab (1984) Matlab. The Mathworks.inc
- 668 Menke EJ (2020) Series of Jupyter Notebooks Using Python for an Analytical Chemistry  
 669 Course. *J Chem Educ* 97:3899–3903. <https://doi.org/10.1021/acs.jchemed.9b01131>
- 670 Mouahid A, Boivin P, Diaw S, Badens E (2022) Widom and extrema lines as criteria for  
 671 optimizing operating conditions in supercritical processes. *J Supercrit Fluids* 186:105587.  
 672 <https://doi.org/10.1016/J.SUPFLU.2022.105587>
- 673 Murtagh F (1991) Multilayer perceptrons for classification and regression. *Neurocomputing*  
 674 2:183–197. [https://doi.org/10.1016/0925-2312\(91\)90023-5](https://doi.org/10.1016/0925-2312(91)90023-5)
- 675 Oliphant TE (2006) Guide to numpy, 2nd edn. Continuum Press
- 676 Pedregosa F, Michel V, Grisel O, et al (2011) Scikit-learn: Machine learning in Python. *Journal  
 677 of Machine Learning Research* 12:2825–2830. [https://doi.org/http://scikit-learn.sourceforge.net/](https://doi.org/http://scikit-<br/>
  678 learn.sourceforge.net/)

- 679 Rai A, Punase KD, Mohanty B, Bhargava R (2014) Evaluation of models for supercritical fluid  
 680 extraction. *Int J Heat Mass Transf* 72:274–287.  
 681 <https://doi.org/10.1016/j.ijheatmasstransfer.2014.01.011>
- 682 Reddy SN, Madras G (2011) A new semi-empirical model for correlating the solubilities of  
 683 solids in supercritical carbon dioxide with cosolvents. *Fluid Phase Equilib* 310:207–212.  
 684 <https://doi.org/10.1016/j.fluid.2011.08.021>
- 685 Roach L, Rignanese G, Fluids AE... of S, 2023 undefined (2023) Applications of machine  
 686 learning in supercritical fluids research. Elsevier 202:896–8446.  
 687 <https://doi.org/10.1016/j.supflu.2023.106051>
- 688 Rovenski V (2010) Modeling of Curves and Surfaces with MATLAB®. Springer New York,  
 689 New York, NY
- 690 Schilling N, Wistuba M, Drumond L, Schmidt-Thieme L (2015) Hyperparameter optimization  
 691 with factorized multilayer perceptrons. Lecture Notes in Computer Science (including  
 692 subseries Lecture Notes in Artificial Intelligence and Lecture Notes in Bioinformatics)  
 693 9285:87–103. [https://doi.org/10.1007/978-3-319-23525-7\\_6](https://doi.org/10.1007/978-3-319-23525-7_6)
- 694 Schneider GM (1978) Physicochemical Principles of Extraction with Supercritical Gases.  
 695 Angewandte Chemie International Edition in English 17:716–727.  
 696 <https://doi.org/10.1002/anie.197807161>
- 697 Schweidtmann AM, Esche E, Fischer A, et al (2021) Machine Learning in Chemical  
 698 Engineering: A Perspective. *Chemie Ingenieur Technik* 93:2029–2039.  
 699 <https://doi.org/10.1002/cite.202100083>
- 700 Selvaratnam B, Koodali RT (2021) Machine learning in experimental materials chemistry.  
 701 *Catal Today* 371:77–84. <https://doi.org/10.1016/j.cattod.2020.07.074>
- 702 Smola AJ, Schölkopf B (2004) A tutorial on support vector regression. *Stat Comput* 14:199–  
 703 222. <https://doi.org/10.1023/B:STCO.0000035301.49549.88>
- 704 Soleimani Lashkenari M, KhazaiePoul A (2017) Application of KNN and Semi-Empirical  
 705 Models for Prediction of Polycyclic Aromatic Hydrocarbons Solubility in Supercritical  
 706 Carbon Dioxide. *Polycycl Aromat Compd* 37:415–425.  
 707 <https://doi.org/10.1080/10406638.2015.1129976>
- 708 Tabernero A, del Valle EMM, Galán MÁ (2010) A comparison between semiempirical  
 709 equations to predict the solubility of pharmaceutical compounds in supercritical carbon  
 710 dioxide. *Journal of Supercritical Fluids* 52:161–174.  
 711 <https://doi.org/10.1016/j.supflu.2010.01.009>
- 712 Tsirikoglou P, Abraham S, Contino F, et al (2017) A hyperparameters selection technique for  
 713 support vector regression models. *Appl Soft Comput* 61:139–148.  
 714 <https://doi.org/10.1016/j.asoc.2017.07.017>
- 715 W McKinney (2011) pandas: a foundational Python library for data analysis and statistics.  
 716 Python for high performance and scientific computing, . <https://doi.org/http://pandas.pydata.org/pandas.html>
- 717 Yamini Y, Moradi M (2011) Measurement and correlation of antifungal drugs solubility in pure  
 718 supercritical CO<sub>2</sub> using semiempirical models. *Journal of Chemical Thermodynamics*  
 719 43:1091–1096. <https://doi.org/10.1016/j.jct.2011.02.020>
- 720